

Coloured-photon antibunching from an out-of-equilibrium condensate

Blanca Silva,^{1,2} Alejandro González Tudela,³ Carlos Sánchez Muñoz,¹ Dario Ballarini,² Milena de Giorgi,² Giuseppe Gigli,² Kenneth W. West,⁴ Loren Pfeiffer,⁴ Elena del Valle,¹ Daniele Sanvitto,² and Fabrice P. Laussy¹

¹*Departamento de Física Teórica de la Materia Condensada, Universidad Autónoma de Madrid, E-28049 Madrid, Spain*

²*NNL, Istituto Nanoscienze – CNR, 73100 Lecce, Italy*

³*Max-Planck Institut für Quantenoptik, 85748 Garching, Germany*

⁴*Department of Electrical Engineering, Princeton University, Princeton, New Jersey 08544, USA*

(Dated: December 3, 2024)

PACS numbers: 42.50.-p, 42.50.Ar, 67.10.-j, 03.65.Yz, 03.75.Nt

Photon correlations are the basic conveyor of optical information in the quantum information age¹. By regulating a stream of photons and/or endowing them with quantum correlations such as entanglement, one can use them as qubits or to distribute cryptographic keys². Every time that a platform demonstrates its ability to generate photons that have such correlations, new prospects arise to extend the frontiers of quantum technology. One rising star to engineer quantum states in solid state optics are microcavity polaritons³. These semiconductor heterostructures can trap both light (cavity photons) and matter (electron-hole pairs) to keep them under strong interaction for a long time. The resulting eigenstates, polaritons, have had resounding successes in the investigation of quantum phases such as Bose–Einstein condensates⁴, superfluids⁵ and nonlinear quantum fluids⁶. They also progress quickly to implement actual devices⁷. Lately, their quantum character was consolidated by the observation of squeezing⁸, indicating nonclassical features at a macroscopic level. Only missing to the polariton prize list is quantum correlation at the single particle level. In this Letter, we report the observation of single-photon antibunching from the emission of an out-of-equilibrium Bose–Einstein condensate. This is made possible thanks to generalized photon correlations that preserve the energy information as well as their time of detection⁹. The success of this technique and its results open the era of quantum polaritonics in microcavities and demonstrate the concept of a new class of quantum correlations that can be pursued in a wide range of optical platforms.

Since the seminal experiment of intensity correlations by Hanbury Brown and Twiss¹⁰, that revolutionized the field of quantum optics and led to Glauber’s Nobel prize for the theory of optical coherence in a quantum setting¹¹, the standard approach to quantify photon correlations is through correlators of the type:

$$g^{(2)}(\tau) = \lim_{t \rightarrow \infty} \frac{\langle a^\dagger(t)a^\dagger(t+\tau)a(t+\tau)a(t) \rangle}{\langle a^\dagger(t)a(t) \rangle \langle a^\dagger(t+\tau)a(t+\tau) \rangle} \quad (1)$$

with $a(t)$ the light field annihilation operator at time t and τ the time delay between detections. This quantity—the second-order correlation function—describes the statistical distribution between photons in their stream of temporal detection. Other properties of the photons can be included, e.g., their position^{10,12} or polarization¹³, with applications spanning from subatomic interferometry¹⁴ to entangled photon pairs generation². One can also record the energy of the photon (or, equivalently, its frequency). This is a characterization of a different type than position or polarization since time and frequency are conjugate variables. It provides as much information as can be retrieved according to quantum mechanics^{9,15,16}. Experimentally, such measurements have been performed for fixed sets of frequencies, by inserting filters in the paths of a standard Hanbury Brown–Twiss setup^{17–21}. Considerably more information is gained, however, by spanning over all possible combinations of frequencies, as this reveals rich landscapes of correlations²² that are washed out when averaging over the energy.

In this Letter, we introduce a technique using a streak camera setup that allows to image such a full mapping of time and frequency resolved photon correlations of an out-of-equilibrium condensate. We use the photon stream coming from a polariton condensate due to the intrinsic importance of Bose–Einstein condensation, which defines the fifth state of matter, as well as for the nontrivial—even unsuspected—features predicted by the theory. Both the principle and the technique are general and should allow, with optimized setups, to revisit systematically all of quantum optics in systems with stronger quantum optical features but weaker intensities of emission. The rich and varied correlation landscapes predicted by the theory²² should be useful to power tomorrow’s quantum technology²³.

The measurement is sketched in Fig. 1(a) and is detailed in the Methods section. To summarize the basics: light is dispersed by a monochromator and is directed into a streak camera that operates at the single-photon level, as has already been demonstrated with standard photon correlations under pulsed excitation²⁴. The sweeping in time and dispersion in energy allow the simultaneous recording of both the time and frequency of

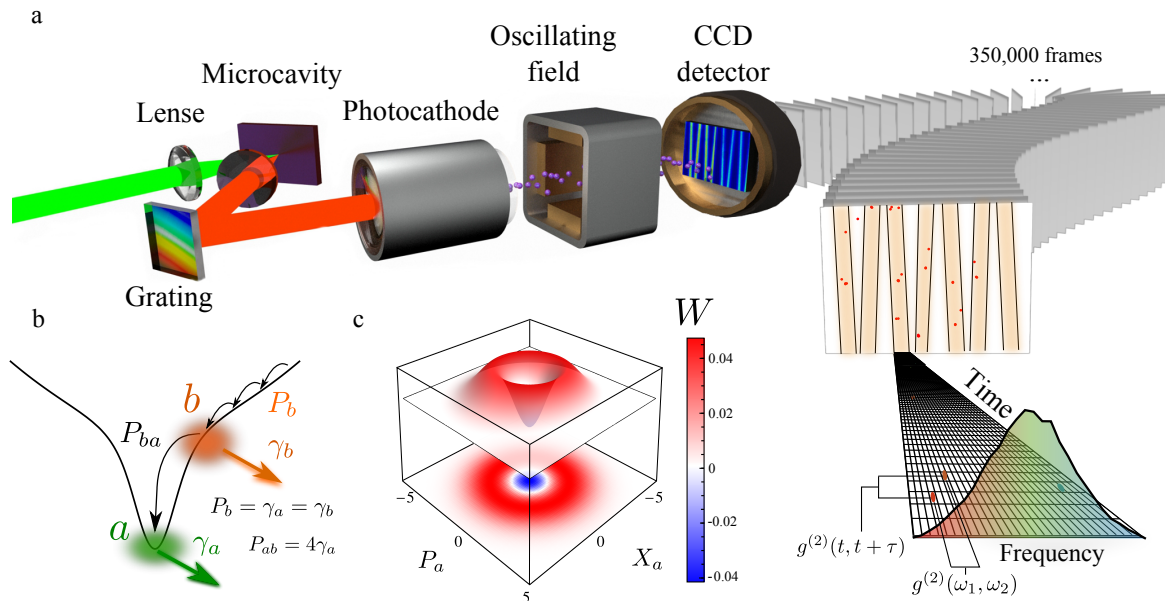


FIG. 1: **Principle and Setup of time- and frequency-resolved photon correlations.** (a) Sketch of the experiment: the reflected light from a microcavity is dispersed onto a streak-camera detecting at the single-photon level and stored in individual frames which post-processing allows to build photon-correlation landscapes (b) Sketch of the theory: a laser excites non-resonantly the lower polariton dispersion, creating a reservoir of hot excitons b that condense into the ground state a at the minimum of the branch. (c) Theoretical Wigner function of the condensate in the steady state regime of out-of-equilibrium condensation: the Wigner function takes negative values (blue region), which proves the genuine quantum nature of the state.

each detected photon in successive frames that are post-processed to calculate intensity correlations. A scheme of the system is shown in Fig. 1(b): polaritons condense into the ground state from a reservoir of high energy polaritons injected by a CW off-resonant laser. There are constant losses, chiefly through the cavity mirror, which allow to study the steady-state correlations. The reservoir relaxation into the condensate is typically phonon-mediated and establishes a nontrivial quantum coherence between the two systems,²⁵ that is responsible for the spontaneous coherence buildup²⁶. The main experimental signature of polariton condensation is line narrowing with increasing pumping as the system goes from a chaotic source to a coherent one. In standard photon correlation measurements, this results in a transition of $g^{(2)}(0)$ from above 1 to 1,^{25,27}. However, none of these features guarantee quantum correlations at the single particle level. On the other hand, such an out-of-equilibrium condensate is effectively able to sustain a quantum correlated steady state when the condensate is not fully formed and is in its stage of coherence buildup. This is demonstrated by, e.g., the Wigner function of the condensate, which is a representation of the state in the phase space of quadratures that proves its quantum character whenever it takes negative values. Its theoretical calculation for our regime of condensation is shown in Fig. 1(c) and does, indeed, correspond to a genuine quantum state.

The quantum character also manifests in direct two-photon correlations when keeping the energy degrees of

freedom. The so-called “two-photon correlation spectrum” $g_{\Gamma}^{(2)}(\omega_1, \omega_2; \tau)$ provides the tendency of a photon to be detected at a frequency ω_2 at a delay τ after another photon has been detected at frequency ω_1 ^{9,22}. Each photon is detected within a frequency window of size Γ . The theoretical calculation is shown for photon coincidences ($\tau = 0$) in Fig. 2(a) in the regime where the condensate is maintained in its nucleating stage in a steady state thanks to the out of equilibrium character of polaritons. One sees that on the diagonal of equal-frequency detection, the theory predicts bunching. This is true even for cases when the overall stream is uncorrelated, as such a bunching induced by frequency filtering is a general result linked to Purcell’s argument of the Bose character of the field²⁸. More interestingly, when correlating photons with opposite frequencies, the theory predicts correlation that exhibits a clear antibunching ($g^{(2)}(\omega_1, \omega_2; 0) < 1$), i.e., detecting a photon on one side of the spectrum makes it less likely to detect another photon on the other side. For stationary processes, such an antibunching of coloured photons is observed for systems with a nonlinearity at the single particle level²², e.g., a two-level system. For a state undergoing condensation, such an antibunching is a priori unexpected. It can be understood on physical grounds as a manifestation of the exchange energy term that makes bosons effectively attract each other. In the regime of their condensation, particles exhibit a transition towards a collective state with which they share identical features, resulting in the antibunching of particles with too distinct characteris-

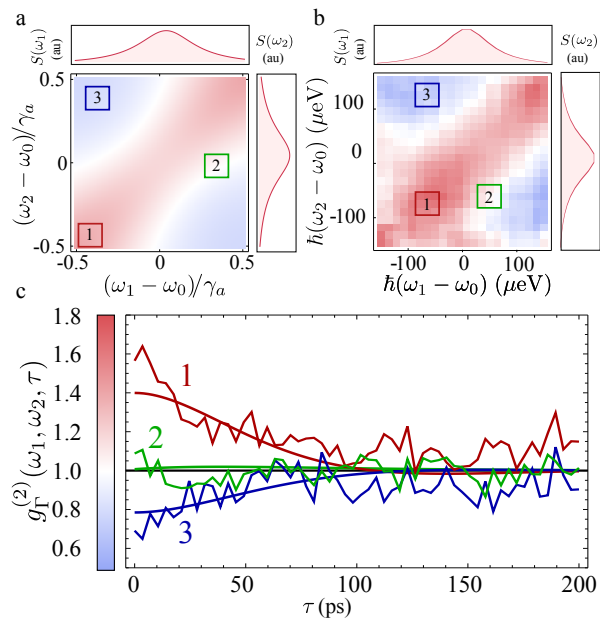


FIG. 2: **Two-photon correlations spectra.** (a) Theoretical calculation of $g^{(2)}(\omega_1, \omega_2; 0)$ in the regime of out-of-equilibrium condensation, predicting regions of frequency antibunching (blue). (b) Experimental observation of $g^{(2)}(\omega_1, \omega_2; 0)$ in the same regime, displaying a remarkable agreement. (c) Time-resolved correlation for the three regions marked in the colour map: (i) on the diagonal ($\omega_1 = \omega_2$) exhibiting bunching, (ii) in the region of transition with no correlation, (iii) correlating opposing elbows, exhibiting antibunching.

tics.

With the procedure described previously, we are able to obtain $g^{(2)}(\omega_1, \omega_2; \tau)$ experimentally. In Fig. 2b, we show the experimental $\tau = 0$ two-photon correlations spectrum measured for the polariton condensate. An excellent agreement with the theory is obtained: same frequency photons are bunched and, remarkably, the anti-diagonal also features two clear regions of antibunching where $g^{(2)}(\omega_1, \omega_2; \tau = 0) < 1$. This is, to the best of our knowledge, the first time that a polariton system exhibits from a macroscopic phase a quantum behaviour at the single particle level. The data required prolonged acquisition times in extremely stable conditions to collect millions of events to reconstruct the landscape of quantum correlations, and although they have some level of noise, the features are unambiguous. In Fig. 2c, we show the temporal correlations for three points of the (ω_1, ω_2) -space, both for the experiment and the theoretical model. Again, there is an extremely good agreement and a clear evolution of the correlations from bunching ($g^{(2)}(\omega, \omega; 0) \approx 1.5$ in region 1) to antibunching ($g^{(2)}(-\omega, \omega; 0) \approx 0.7$ in region 3). Another fundamental feature of the theory is that correlations depend on the frequency windows that select which photons are correlated. Smaller windows lead to stronger correlations but, again, at the price of a smaller signal. In Fig. 3, we show

the dependence of the two-photon correlation spectrum on the size of the frequency windows for a point that features antibunching. When the frequency window is very large, $\Gamma \gg \gamma_a$, both the experimental and theoretical $g^{(2)}(\omega_1, \omega_2; \tau)$ recover as expected the results of standard photon correlations which has always been reported to be larger than 1 for these kinds of systems. As the size of the frequency window decreases, the system shows a transition from bunching to antibunching, demonstrating how single-photon antibunching can be uncovered simply by discriminating in frequency. The observation matches again extremely well with the theory.

At this point it is important to put these results in perspective with the canon of quantum optics and the pre-existing findings. There are various indicators of the quantum nature of a system, such as violation of Cauchy–Schwarz inequalities or Bell’s inequalities, also for coloured photons²⁹. In our case, the quantum character does not manifest in these terms, i.e., through a conventional antibunching $g^{(2)}(0) < g^{(2)}(\tau) \leq 1$, or its multimode counterpart. Our findings are also different from squeezing, which is not present in the model of out-of-equilibrium Bose-Einstein Condensation. The quantum character is however established theoretically from the unmistakable criterion provided by the Wigner function, Fig. 1c. In fact, frequency-resolved photon correlations provide a new indicator for the quantum nature of a system, that is straightforwardly implemented with standards optical laboratory equipment, and should allow to track quantum behaviours in a large family of systems where these are feeble, fragile or washed out by averaging.

As a conclusion, we have established that the photon statistics from the light emitted by a condensate of exciton-polariton in the dynamical process of condensation exhibits quantum correlations. These are not directly apparent if considering all photons indiscriminately as competing correlations exist between photons of different frequencies. This results in the washing out of a considerable amount of information. We have demonstrated the possibility to extract the correlation landscapes experimentally and found an excellent agreement with the theory. This shows that both the theoretical concepts and the experimental technique are robust and ripe to be deployed in a large range of quantum optical systems, with prospects of evidencing further classes of quantum correlations and optimizing those already known. Systems such as superconducting qubits, that have achieved an impressive control of conventional quantum correlations³⁰, should be able to extend this technique to unravel the much richer quantum landscapes sculpted in the light field by a two-level system²².

Methods

Experiments: The sample is a semiconductor microcavity with high reflective Bragg mirrors and 3×4 quan-

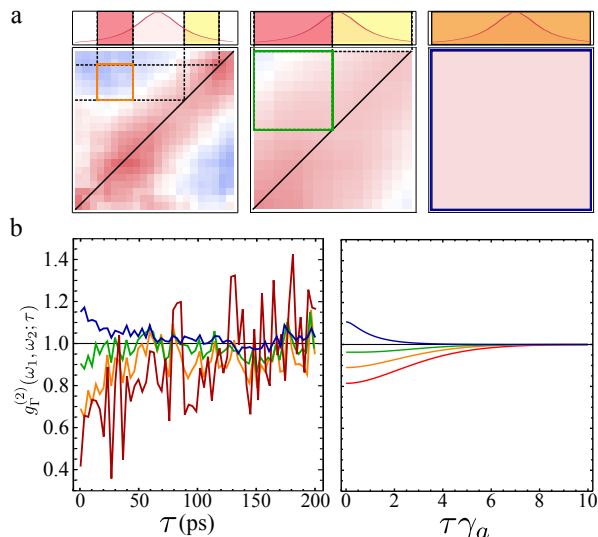


FIG. 3: **Effect of detectors linewidths.** (a) two-photon correlation landscapes $g^{(2)}(\omega_1, \omega_2; 0)$ as a function of the filter width, from a fraction of the peak, $74.1 \mu\text{eV}$ (left), roughly half-peak width, $158.8 \mu\text{eV}$ (center), to full-peak filtering, corresponding to standard auto-correlations. The position of the two filters is shown explicitly on the spectral line as the red and yellow windows (orange when overlapping). (b) Time-resolved traces for the selected areas. The smallest frequency window available, $10.6 \mu\text{eV}$, is shown in red: antibunching is even more pronounced although the signal becomes extremely noisy.

tum wells at the antinodes of a 2λ cavity. It is pumped at normal incidence and non-resonantly with a single-mode laser at a wavelength of 725.2 nm . Each photon emitted by the lower polariton state is mapped to a pixel in the streak detector with a temporal and spectral resolution of 3.2 ps and $70 \mu\text{eV}$ respectively in a total window of $1536 \text{ ps} \times 456.7 \mu\text{eV}$. The correlation landscapes are obtained from correlations between these clicks (≈ 1.69 per sweep in a total of $350\,000$ frames). We found it important not to use a chopper, that introduces long timescales correlations due to heating and cooling of the sample that result in non-stationarity of the photon statistics, although this is not apparent through single-photon observables such as the intensity. This, of course, limits the

range of excitation power we can use. The widths in frequency are defined while computing the correlations by grouping consecutive pixels in windows of different sizes with a minimum step size of $10.6 \mu\text{eV}$. Two-photon correlation spectra are obtained by spanning the windows to compute all possible correlations, including partial and full-overlapping of the windows. This shows the considerable improvement of a streak-camera over standard setups with APDs. All the computations are done with the raw data only: there is no normalization and the correlations go to 1 at long time self-consistently.

Theory: The quantum dynamics of an out-of-equilibrium condensate maintained in a steady state through the interplay of pump and decay is described at its most elementary level through the master equation (see Supplementary Information online):

$$\frac{\partial \rho}{\partial t} = \left[\frac{\gamma_a}{2} \mathcal{L}_a + \frac{\gamma_b}{2} \mathcal{L}_b + \frac{P_b}{2} \mathcal{L}_{b^\dagger} + \frac{P_{ba}}{2} \mathcal{L}_{a^\dagger b} \right] (\rho). \quad (2)$$

with Lindblad terms $\mathcal{L}_O(\rho) = 2O\rho O^\dagger - O^\dagger O\rho - \rho O^\dagger O$ for any operator O , corresponding to the polariton condensate a and reservoir b lifetimes, reservoir pumping b^\dagger and particles transfer $a^\dagger b$ from the reservoir to the condensate. Parameters are $\gamma_a = \gamma_b$ throughout and $P_{ba} = 10\gamma_a$ except for Fig. 1 where $P_{ba} = 4\gamma_a$ (the Wigner is still negative at $P_{ba} = 4\gamma_a$). The filter linewidth is $\Gamma = \gamma_a/2$ throughout except in Fig. 3 where it spans $\Gamma \in \{0.5, 0.75, 1, 5\}\gamma_a$. The reservoir pumping $P_b = \gamma_b$ throughout except Fig. 2 where it is also $2\gamma_b$. The quantum state of the reduced density matrix $\rho_a = \text{Tr}_b(\rho)$ can be computed in the Wigner function form, i.e., as a phase-space distribution in the quadratures $X_a = a^\dagger + a$ and $P_a = i(a^\dagger - a)$ of the field (cf. Supplementary Information online). The two-photon correlations resolved in frequency in windows of linewidth Γ reads⁹:

$$g_{\Gamma}^{(2)}(\omega_1, T_1; \omega_2, T_2) = \frac{\langle : \mathcal{T} [\prod_{i=1}^2 A_{\omega_i, \Gamma}^\dagger(T_i) A_{\omega_i, \Gamma}(T_i)] : \rangle}{\prod_{i=1}^2 \langle A_{\omega_i, \Gamma}^\dagger(T_i) A_{\omega_i, \Gamma}(T_i) \rangle} \quad (3)$$

with \mathcal{T} , (resp. $:$) the time (resp. normal) ordering and $A_{\omega_i, \Gamma}(T_i) = \int_{-\infty}^{T_i} e^{i\omega_i t} e^{-\Gamma(T_i-t)/2} a(t) dt$ the field filtered at frequency ω_i and width Γ at a time T_i .

-
- [1] Nielsen, M. A. & Chuang, I. L. *Quantum computation and quantum information* (Cambridge university press, 2010).
 [2] Ekert, A. K. Quantum cryptography based on bell's theorem. *Phys. Rev. Lett.* **67**, 661 (1991).
 [3] Kavokin, A., Baumberg, J. J., Malpuech, G. & Laussy, F. P. *Microcavities* (Oxford University Press, 2011), 2 edn.
 [4] Kasprzak, J. *et al.* Bose–Einstein condensation of exciton polaritons. *Nature* **443**, 409 (2006).
 [5] Amo, A. *et al.* Collective fluid dynamics of a polariton

condensate in a semiconductor microcavity. *Nature* **457**, 291 (2009).

- [6] Amo, A. *et al.* Polariton superfluids reveal quantum hydrodynamic solitons. *Science* **332**, 1167 (2011).
 [7] Ballarini, D. *et al.* All-optical polariton transistor. *Nat. Comm.* **4**, 1778 (2013).
 [8] Boulier, T. *et al.* Polariton-generated intensity squeezing in semiconductor micropillars. *Nat. Comm.* **5** (2014).
 [9] del Valle, E., Gonzalez-Tudela, A., Laussy, F. P., Tejedor, C. & Hartmann, M. J. Theory of frequency-filtered and time-resolved n -photon correlations. *Phys. Rev. Lett.*

- 109, 183601 (2012).
- [10] Hanbury Brown, R. & Twiss, R. Q. A test of a new type of stellar interferometer on Sirius. *Nature* **178**, 1046 (1956).
- [11] Glauber, R. J. Nobel lecture: One hundred years of light quanta. *Rev. Mod. Phys.* **78**, 1267 (2006).
- [12] Weiner, R. M. *Introduction to Bose-Einstein Correlations and Subatomic Interferometry* (John Wiley & Sons Inc, 2000).
- [13] Stevenson, R. M. *et al.* A semiconductor source of triggered entangled photon pairs. *Nature* **439**, 179 (2006).
- [14] Jeltjes, T. *et al.* Comparison of the Hanbury Brown–Twiss effect for bosons and fermions. *Nature* **445**, 402 (2007).
- [15] Cohen-Tannoudji, C. & Reynaud, S. Atoms in strong light-fields: Photon antibunching in single atom fluorescence. *Phil. Trans. R. Soc. Lond. A* **293**, 223 (1979).
- [16] Nienhuis, G. Spectral correlations in resonance fluorescence. *Phys. Rev. A* **47**, 510 (1993).
- [17] Akopian, N. *et al.* Entangled photon pairs from semiconductor quantum dots. *Phys. Rev. Lett.* **96**, 130501 (2006).
- [18] Hennessy, K. *et al.* Quantum nature of a strongly coupled single quantum dot–cavity system. *Nature* **445**, 896 (2007).
- [19] Kaniber, M. *et al.* Investigation of the nonresonant dot-cavity coupling in two-dimensional photonic crystal nanocavities. *Phys. Rev. B* **77**, 161303(R) (2008).
- [20] Sallen, G. *et al.* Subnanosecond spectral diffusion measurement using photon correlation. *Nat. Photon.* **4**, 696 (2010).
- [21] Ulhaq, A. *et al.* Cascaded single-photon emission from the Mollow triplet sidebands of a quantum dot. *Nat. Photon.* **6**, 238 (2012).
- [22] Gonzalez-Tudela, A., Laussy, F. P., Tejedor, C., Hartmann, M. J. & del Valle, E. Two-photon spectra of quantum emitters. *New J. Phys.* **15**, 033036 (2013).
- [23] Sanchez Muñoz, C. S. *et al.* Emitters of n -photon bundles. *Nat. Photon.* (2014).
- [24] Wiersig, J. *et al.* Direct observation of correlations between individual photon emission events of a microcavity laser. *Nature* **460**, 245 (2009).
- [25] Laussy, F. P., Malpuech, G., Kavokin, A. & Bigenwald, P. Spontaneous coherence buildup in a polariton laser. *Phys. Rev. Lett.* **93**, 016402 (2004).
- [26] Holland, M., Burnett, K., Gardiner, C., Cirac, J. I. & Zoller, P. Theory of an atom laser. *Phys. Rev. A* **54**, R1757 (1996).
- [27] Deng, H., Weihs, G., Santori, C., Bloch, J. & Yamamoto, Y. Condensation of semiconductor microcavity exciton polaritons. *Science* **298**, 199 (2002).
- [28] Purcell, E. M. The question of correlation between photons in coherent light rays. *Nature* **178**, 1449 (1956).
- [29] Reid, M. D. & Walls, D. F. Violations of classical inequalities in quantum optics. *Phys. Rev. A* **34**, 1260 (1986).
- [30] Lang, C. *et al.* Observation of resonant photon blockade at microwave frequencies using correlation function measurements. *Phys. Rev. Lett.* **106**, 243601 (2011).

Acknowledgements

We thank Guillermo Guirales Arredondo for assistance with Fig. 1. This work has been funded by the ERC Grant POLAFLOW and the IEF project SQUIRREL (623708). AGT acknowledges support from the Alexander Von Humboldt Foundation, C.S.M. from a FPI grant and F.P.L. a RyC contract.